

The energy spectrum of cosmic rays in the range from 10^{14} to $10^{18}\,\mathrm{eV}$

S. Schoo*1, W.D. Apel1, J.C. Arteaga-Velázquez2, K. Bekk1, M. Bertaina3,

J. Blümer^{1,4}, H. Bozdog¹, I.M. Brancus⁵, E. Cantoni^{3,6}, A. Chiavassa³, F. Cossavella⁴,

K. Daumiller¹, V. de Souza⁷, F. Di Pierro³, P. Doll¹, R. Engel¹, D. Fuhrmann⁸,

A. Gherghel-Lascu⁵, H.J. Gils¹, R. Glasstetter⁸, C. Grupen⁹, A. Haungs¹, D. Heck¹,

J.R. Hörandel¹⁰, D. Huber⁴, T. Huege¹, K.-H. Kampert⁸, D. Kang⁴, H.O. Klages¹,

K. Link⁴, P. Łuczak¹¹, H.J. Mathes¹, H.J. Mayer¹, J. Milke¹, B. Mitrica⁵, C. Morello⁶,

J. Oehlschläger¹, S. Ostapchenko¹², N. Palmieri⁴, T. Pierog¹, H. Rebel¹, M. Roth¹,

H. Schieler¹, F.G. Schröder¹, O. Sima¹³, G. Toma⁵, G.C. Trinchero⁶, H. Ulrich¹,

A. Weindl¹, J. Wochele¹, J. Zabierowski¹¹ - KASCADE-Grande Collaboration

The KASCADE experiment and its extension KASCADE-Grande have significantly contributed to the current knowledge about the energy spectrum and composition of cosmic rays (CRs) with energies between the knee and the ankle. However, the data of both experiments were analysed separately, although Grande used the muon information of the KASCADE-array. A coherent analysis based on the combined data of both arrays is expected to profit from reconstructed shower observables with even higher accuracy compared to the stand-alone analyses. In addition, a significantly larger fiducial area is available.

By this analysis we obtain the spectrum and composition of CRs in the range from 10^{14} to $10^{18}\,\mathrm{eV}$ with a larger number of events and further reduced uncertainties using one unique reconstruction procedure for the entire energy range. This contribution will provide an outline of the reconstruction procedure used and the preliminary energy spectrum and composition obtained will be presented.

The 34th International Cosmic Ray Conference, 30 July- 6 August, 2015 The Hague, The Netherlands

¹ Institut für Kernphysik, KIT - Karlsruhe Institute of Technology, Germany

² Universidad Michoacana, Inst. Física y Matemáticas, Morelia, Mexico

³ Dipartimento di Fisica, Università degli Studi di Torino, Italy

⁴ Institut für Experimentelle Kernphysik, KIT - Karlsruhe Institute of Technology, Germany

⁵ Horia Hulubei National Institute of Physics and Nuclear Engineering, Bucharest, Romania

⁶ Osservatorio Astrofisico di Torino, INAF Torino, Italy

⁷ Universidade São Paulo, Instituto de Física de São Carlos, Brasil

⁸ Fachbereich Physik, Universität Wuppertal, Germany

⁹ Department of Physics, Siegen University, Germany

¹⁰ Dept. of Astrophysics, Radboud University Nijmegen, The Netherlands

¹¹ National Centre for Nuclear Research, Department of Astrophysics, Lodz, Poland

¹² Frankfurt Institute for Advanced Studies (FIAS), Frankfurt am Main, Germany

¹³ Department of Physics, University of Bucharest, Bucharest, Romania E-mail: sven.schoo@kit.edu

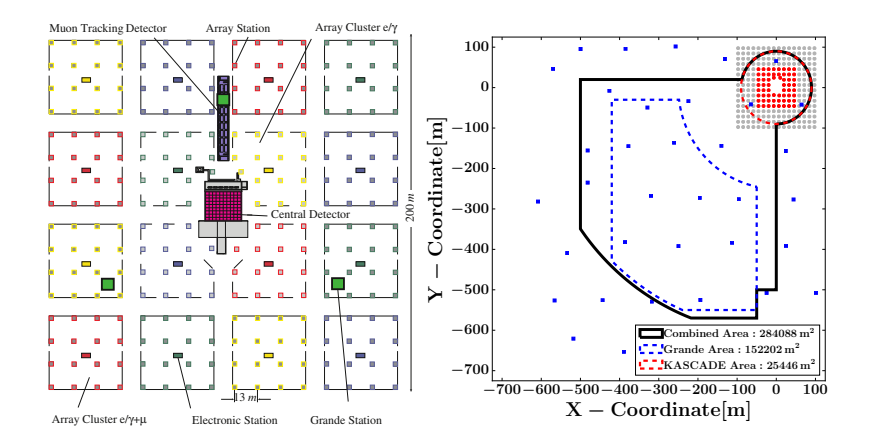


Figure 1: The layout of the KASCADE experiment is shown in the left picture. Each station was equipped with shielded and non-shielded scintillators, except for the stations of the inner four clusters, which were installed without the shielded scintillators, but with twice as many non-shielded ones (See [1]). In the right plot, the stations of the KASCADE-Grande array (rectangles) are shown relative to the KASCADE array. They have been equipped with non-shielded detectors only. In addition, the fiducial areas used for the two standalone reconstructions and the combined analysis are shown.

1. Outline

Up to now the KASCADE [1] and KASCADE-Grande [2] recordings have been analyzed independently of each other. The next two sections will provide a basic overview of the setups and reconstruction procedures for the KASCADE and KASCADE-Grande arrays. The third section will show the benefits from combining both detector setups in terms of the reconstruction accuracy of the number of electrons (N_e) and the number of muons (N_μ). The last section is dedicated to the reconstructed energy spectrum. It will show that the combined array can indeed cover an energy range spanning more than 3 orders of magnitude.

2. KASCADE

The KASCADE experiment was located in Karlsruhe (Lon.: 8.4° , Lat.: 49.1°), Germany at an altitude of approximately 110 m a.s.l. The layout of the experiment with the array, the muon tracking detector and the central detector is shown on the left hand side (l.h.s.) of Fig. 1. The array consisted of 252 stations organized in 16 clusters. While the 192 stations of the outer 12 clusters were equipped with shielded ($3.24\,\mathrm{m}^2$) and non-shielded ($1.57\,\mathrm{m}^2$) scintillation detectors, the stations in the inner four clusters were built without the shielded scintillators, but with twice the number of e/γ detectors ($3.14\,\mathrm{m}^2$). Using this setup, the simultaneous reconstruction of N_e and N_H is possible.

The number of particles corresponding to a certain energy deposited in a detector is calculated by dividing the total energy deposit by the effective energy deposited per single charged particle taking into account also the energy deposited by photons and the e/γ ratio. This procedure is explained in detail in [3]. N_e is obtained by fitting a NKG-like lateral density function (LDF) [4][5]

^{*}Speaker.

to the particle densities measured at the e/γ detectors. After this step, $N_{\rm e}$ is the number of charged particles. The reconstruction of the number of muons is done simultaneously, therefore, the muon LDF is already known at this stage and the information is included in the next iteration of the fitting procedure for the e/γ detectors resulting in the reconstruction of $N_{\rm e}$ as the number of electrons.

The reconstruction of the number of muons follows the same scheme as the reconstruction of N_e . The transformation of energy deposits to particle densities takes into account the N_e -dependent probability of electrons, photons or hadrons passing the shielding especially near the shower core. This faked muon deposit gets dominant below a distance of 40 m, therefore, stations within this distance to the shower core are excluded from the analysis. In addition, the NKG-like LDF is known to deviate from the true lateral muon distribution towards large core distances, therefore, the muon LDF is integrated only in the range from $40 - 200 \,\mathrm{m}$, where the KASCADE detectors provide sampling points for the fit. The result is the truncated number of muons ($N_u^{\mathrm{tr.}}$).

For a more detailed description of the reconstruction procedure see [3].

3. KASCADE-Grande

KASCADE-Grande was located next to the KASCADE array with an overlap as it is shown on the right hand side (r.h.s.) of Fig. 1. Covering an energy range from 10 PeV up to 1 EeV, there is also an overlap between the energy spectra of both arrays.

The KASCADE-Grande stations were equipped with non-shielded scintillation detectors (10 m² per station) only, therefore, the reconstruction of the number of muons is only possible using the shielded detectors of the KASCADE array.

The energy deposited in the KASCADE-Grande detectors is mainly governed by the distance-dependent γ /e ratio and the energy distribution of electrons and photons. Unlike for the KASCADE array, a dependence on the shower size has been found to be negligible and does not contribute to the transformation of the deposited energy to the number of particles. The LDF used for the electromagnetic component is again a modified NKG-function. The reconstruction of the number of muons, however, is based on a function described by Lagutin and Raikin [6]. The number of muons is reconstructed by using the core position and arrival direction reconstructed using the Grande detectors, therefore, the KASCADE detectors only contribute their measured muon densities. A detailed description can be found in [2].

4. Improving by Combining

After converting the energy deposits to the number of particles using the methods of the standalone analyses, the reconstruction procedure of the combined detector array follows the one described in section 2, however, the mentioned truncation of the muon number is not applied in the combined reconstruction.

In this section the reconstruction accuracies of $N_{\rm e/ch/\mu}$ of the KASCADE and KASCADE-Grande standalone analyses are compared to the accuracies achieved by using both detectors simultaneously. Please note, that the results concerning the combined analysis are to be considered preliminary. The analysis is still ongoing and further improvements are to be expected as the reconstruction procedure is still being carefully optimized. This presentation is, therefore, to be

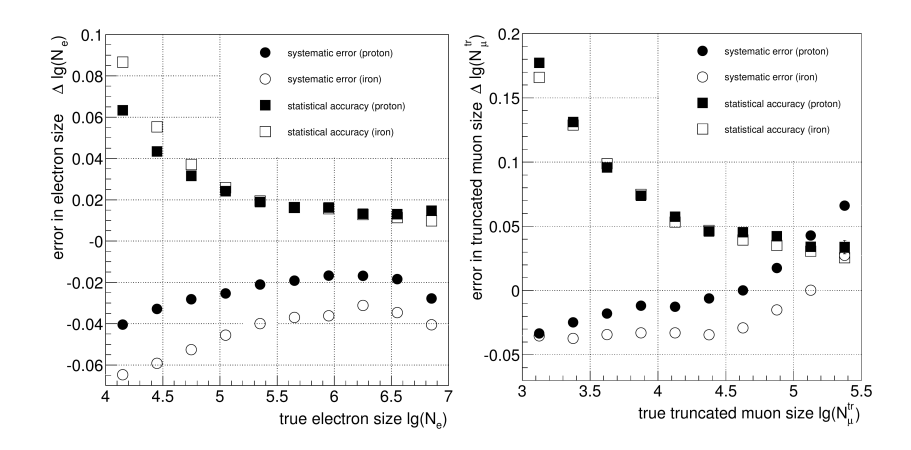


Figure 2: The reconstruction accuracies of KASCADE for N_e (left panel) and N_u (right panel), see [1].

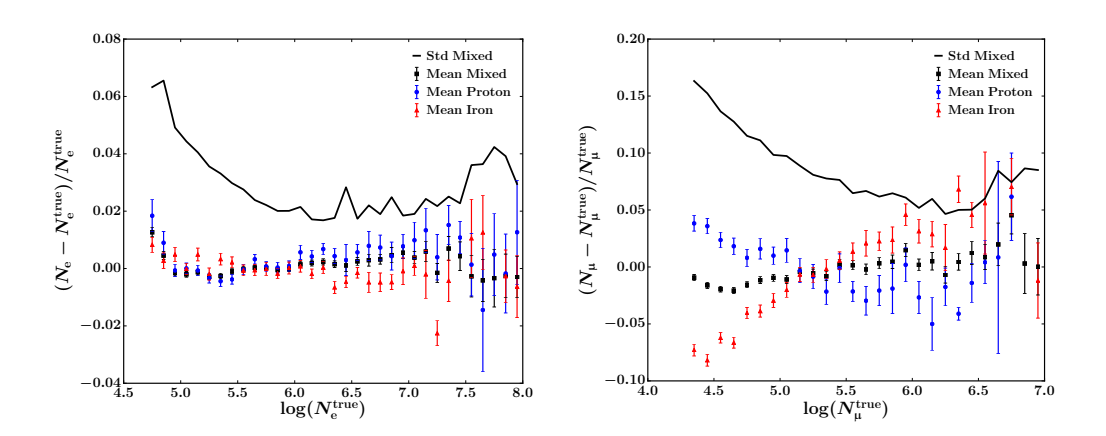


Figure 3: The reconstruction accuracies of KASCADE using the combined reconstruction for N_e (left panel) and N_{μ} (right panel). Note the larger range at the x-axis compared to Fig. 2.

considered as a proof of concept, that by combining the two arrays, the successful reconstruction of showers within an energy range of more than 3 decades is possible.

Fig. 2 shows the accuracies reached for proton and iron induced showers using only the KASCADE array for the reconstruction of $N_{\rm e}$ and $N_{\rm \mu}$. Fig. 3 displays the same information using the combined reconstruction, however, the number of muons has been obtained without the truncation mentioned in section 2 and is, therefore, not 100% comparable. Note, that for KASCADE standalone the difference of $log(N_{\rm e/\mu})$ to their corresponding Monte-Carlo truths is given, while for the combined analysis the difference is shown in percent of the Monte-Carlo truths. The accuracy of $N_{\rm e}$ at 10^5 electrons is about 6% for the array alone, compared to about 4.5% for the combined reconstruction. Both reconstructions reach an accuracy of better than 3% towards higher energies. Above 10^7 electrons, the number of simulated events is too low to reach a reliable estimate. Within the range $10^{4.5} < N_{\mu} < 10^{6.0}$ the reconstruction accuracy improves from around 15% to below 5% for the combined analysis. This range is shifted in log scale by roughly 0.5 units due to the truncation i.e. to $10^{4.0} < N_{\mu}^{\rm trunc} < 10^{5.5}$ for the standalone analysis. Within this range, the accuracy changes from around 17% to below 7%. The improvement in the muon reconstruction due to the

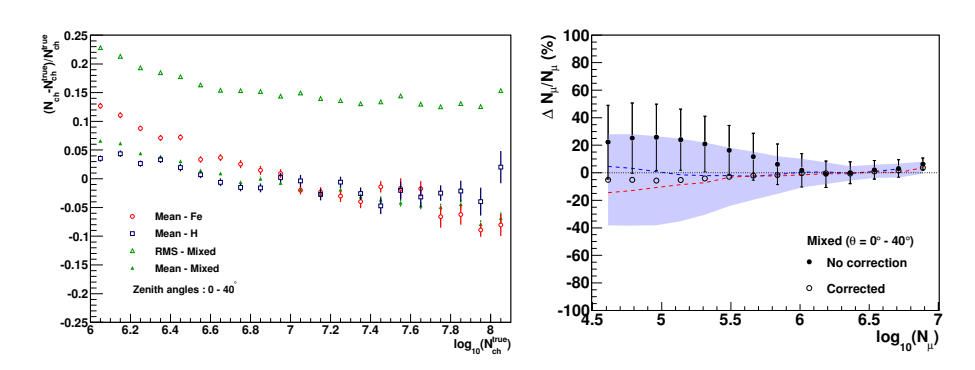


Figure 4: The reconstruction accuracies for KASCADE-Grande for N_{ch} (left panel, See [1]) and N_{μ} (right panel, see [7]).

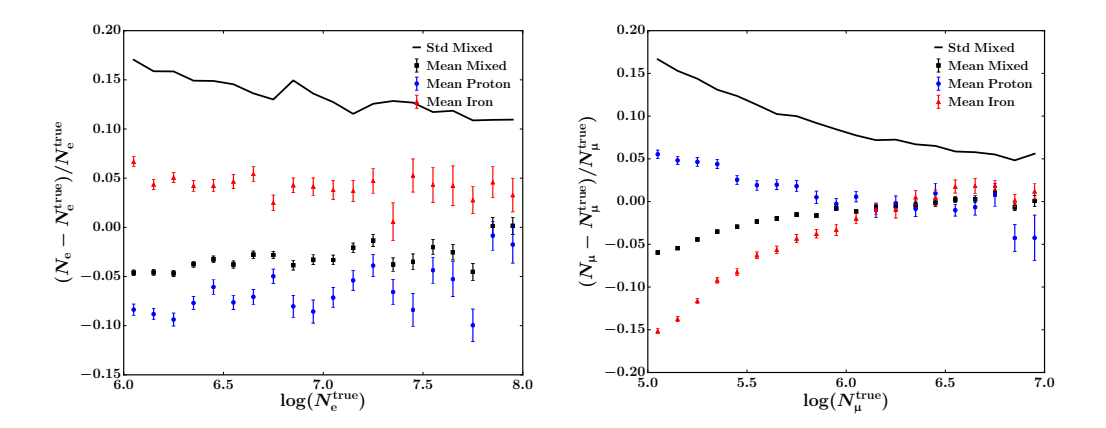


Figure 5: The reconstruction accuracies for KASCADE-Grande using the combined reconstruction for $N_{\rm ch}$ (left panel) and N_{μ} (right panel).

combined use of both detectors is rather small, considering that we are, in principle, comparing two different, although connected, observables.

Fig. 4 shows the accuracies reached using only the KASCADE-Grande array for the reconstruction of $N_{\rm ch}$ and, as described in section 3, the KASCADE array for the reconstruction of $N_{\rm \mu}$. The accuracy for the number of electrons improves from just above 22% to about 15% within the energy range of KASCADE-Grande. At the threshold of full efficiency, i.e. at $10^{5.3}$ muons, the number of muons is reconstructed with an accuracy of about 25%. Towards higher energies, this number decreases to only about 5%.

The corresponding accuracy for the combined reconstruction is shown in Fig. 5. In the same range, $N_{\rm e}$ (instead of $N_{\rm ch}$) is reconstructed with an accuracy of 17% to 11%. Therefore, the combined reconstruction reaches an improved accuracy over the entire range. Also the number of muons is reconstructed more accurately than before. The new procedure reaches an accuracy within $10^{5.3}$ to 10^7 muons of about 14 to 5%.

The combination of the detectors right at the beginning of the reconstruction procedure results in much more accurately estimated observables. This is especially true for KASCADE-Grande, for which an improvement of several percent is achieved.

5. The energy spectrum

Following the procedure further explained in [7], the energy of the primary particle can be estimated on an event-by-event basis using N_e and N_μ . The energy is obtained by using the mean simulated energies for proton and iron primaries as a function of N_e while taking the mass dependence into account based on the ratio of N_e over N_μ , again as a function of N_e . As described in [8, 9], the same mass sensitive ratio can be used to separate the events in two sets - one containing events induced primarily by heavy primaries and the other containing events generated by light particles.

The selected data includes zenith angles between 0 and 30°, however, the analysis is split into three zenith angle ranges to take the shower attenuation into account. Each range is fully efficient above the corresponding chosen minimum energy, the lower zenith angle ranges reaching slightly farther down in energy than the highest one. This is accounted for in the analysis procedure. The combined trigger and reconstruction efficiencies for KASCADE and KASCADE-Grande (for the combined analysis derived using QGSJetII-04 [10] based simulations) are shown in Fig. 6 for the first zenith angle range (0 to 16.7°), since this is the range that can reach farthest down in energy while being fully efficient. It shows, therefore, what should currently be possible if the analysis of lower energetic events is restricted to less inclined showers.

Efficiencies exceeding one are due to the migration of events among the zenith angle ranges and due to events being reconstructed as being located inside the selected area, although they are truly lying outside of it. This effect is not very prominent in the data, neither for the KASCADE area, nor for the KASCADE-Grande part of the chosen area, which is shown in Fig. 1. While for the events located in the Grande array a full efficiency cut at $10^{16}\,\mathrm{eV}$ is applied, it could reach slightly farther down in energy towards $10^{15.7}\,\mathrm{eV}$. Although only the first zenith angle range is shown, the combined array is fully efficient above $10^{16}\,\mathrm{eV}$ for the whole area and the total zenith angle interval. Showers located within the former KASCADE-array, can be efficiently triggered and reconstructed also at energies below $10^{16}\,\mathrm{eV}$. The array being not $100\,\%$ efficient even at $10^{15}\,\mathrm{eV}$ when using the combined analysis is not due to the trigger efficiency of the array, as it was shown already in [1], where the combined trigger and reconstruction efficiency was estimated to be $100\,\%$ already at an energy slightly below $10^{15}\,\mathrm{eV}$. Therefore, it is due to the efficiency of the combined reconstruction procedure, which will be improved for lower energies in order to enable the fully efficient combined reconstruction also at energies towards and below $10^{15}\,\mathrm{eV}$.

It is interesting to note, that even towards $10^{14} \,\mathrm{eV}$ more than half of the simulated events have been successfully triggered and reconstructed and survived all quality cuts. However, a correction for inefficiencies would increase the systematic uncertainties not studied yet, hence, this presentation will be restricted to showers above $10^{15.3} \,\mathrm{eV}$ in the case that the event was located in the former KASCADE array and above $10^{16} \,\mathrm{eV}$ for the rest of the chosen fiducial area.

Next to the improved reconstruction accuracies, one important advantage of the combined reconstruction is the increased distance range for sampling points accessible for events located in the KASCADE array. This is immediately visible in the available energy range which now reaches up to $10^{18}\,\mathrm{eV}$, i.e the upper limit of the KASCADE-Grande array and one decade above the upper limit of the standalone KASCADE analyses.

Fig. 7 shows the resulting energy spectra for simulations (l.h.s.) and measured data (r.h.s.).

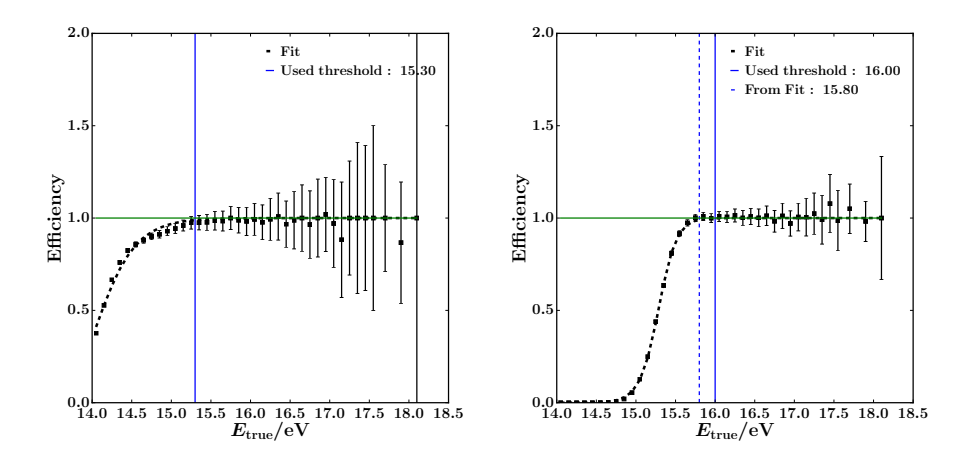


Figure 6: The combined trigger and reconstruction efficiencies for KASCADE (left panel) and KASCADE Grande (right panel) using data with zenith angles between 0.0 and 16.7°.

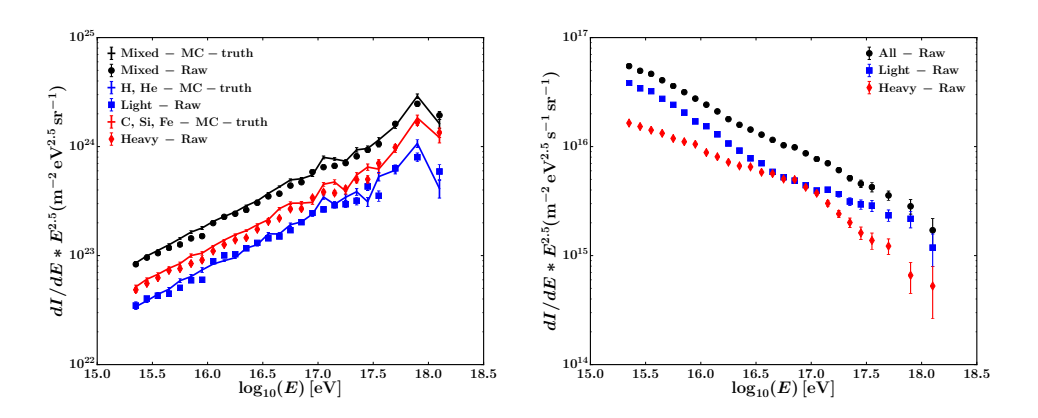


Figure 7: Left: The combined energy spectrum for a mixed composition of H, He, C, Si, and Fe. In addition the results of a separation between predominantly light and heavy events are shown. Spectra labeled with "MC-truth" show the input spectra of the simulations. Right: The raw spectra for all particles, the light, and the heavy component are shown for measured data.

For the simulations, the QGSJetII-04 hadronic interaction model was used. The simulations cover five different primaries, namely protons (H), helium (He), carbon (C), silicon (Si), and iron (Fe), in equal abundances.

Spectra labeled with "MC-truth" correspond to the input spectra of the simulations. Spectra labeled with "Raw" are the results from directly applying the energy reconstruction without any corrections of bin-to-bin migrations. However, due to the spectrum being quite steep, the non-zero bias, and the chosen width of the bins being smaller than the reconstruction accuracy, events will be migrating among the different energy bins. This will be taken into account based on a modified version of an unfolding method proposed by D'Agostini [11].

The bias and accuracy is a bit different for KASCADE and KASCADE-Grande, which is visible at 10¹⁶ eV, below which only events located inside the KASCADE-array are taken into account. For both arrays, the deviation of the reconstructed spectra from the simulated ones show

some dependency on the composition.

For measured data, this cancellation does not work in the same way, since the abundances of heavy and light primaries are different. The approach on the separation will be more sophisticated in the future and, therefore, the dependency on the composition will not be further discussed here. Results for composition assumptions based on calibrations obtained using different hadronic interaction models are shown in [12].

As stated earlier, the uncertainties and known systematics in the energy reconstruction are not taken into account yet. This is one reason why we are showing the current "raw" spectrum alone without adding other spectra obtained by KASCADE, KASCADE-Grande or other experiments. The spectrum will change, once we include the corrections and we do not encourage the usage of the shown spectra for comparisons or model-building.

Nonetheless, the results demonstrate, that the combined reconstruction has reached a state where the consistent combination of both detectors is possible and, in fact, is favorable above the standalone analyses, considering the improved accuracy of the shower observables, the larger fiducial area, and the extended energy range for KASCADE (especially once the reconstruction of low energetic events has been improved).

References

- [1] Antoni T et al. KASCADE-Grande Coll., NIM A 513 (2003) 490
- [2] Apel W D et al. KASCADE-Grande Coll., NIM A 620 (2010) 202
- [3] Apel W D et al. KASCADE-Grande Coll., Astropart. Phys. 24 (2006) 467-483
- [4] Kamata K and Nishimura J, Prog. Theor. Phys. Suppl. 6 (1958) 93-155
- [5] Greisen K, Ann. Rev. Nucl. Sci. 10 (1960) 63-108
- [6] Lagutin A A and Raikin R I Nucl. Phys. Proc. Suppl. 97 (2001) 274
- [7] Apel W D et al. KASCADE-Grande Coll., Astropart. Phys. 36 (2012) 183-194
- [8] Apel W D et al. KASCADE-Grande Coll., Phys. Rev. Lett. 107 (2011) 171104
- [9] Apel W D et al. KASCADE-Grande Coll., Phys. Rev. D 87 (2013) 081101(R)
- [10] Ostapchenko S, Nucl. Phys. B, Proc. Suppl. 151 (2006) 143-146
- [11] D'Agostini G, Nucl. Instr. and Meth. in Phys. Res. A 362 (1995) 487
- [12] Bertaina M et al. KASCADE-Grande Coll., this proceedings (id 359)